Journal of Medicinal Chemistry Article

J. Med. Chem. **2010,** *53,* 5033–5043 **5033**
DOI: 10.1021/jm100274c

Selective Synthesis and Biological Evaluation of Sulfate-Conjugated Resveratrol Metabolites

Juma Hoshino,[†] Eun-Jung Park,[‡] Tamara P. Kondratyuk,[‡] Laura Marler,[‡] John M. Pezzuto,[‡] Richard B. van Breemen,[§] Shunyan Mo,[§] Yongchao Li,[§] and Mark Cushman*,[†]

[†]*Department of Medicinal Chemistry and Molecular Pharmacology, School of Pharmacy and Pharmaceutical Sciences and the Purdue University Center for Cancer Research, Purdue University, West Lafayette, Indiana 47907,* [‡]*College of Pharmacy, University of Hawaii at Hilo, Hilo, Hawaii 96720, and* [§]*University of Illinois College of Pharmacy, 833 S. Wood Street, Chicago, Illinois 60612*

Received March 2, 2010

Five resveratrol sulfate metabolites were synthesized and assessed for activities known to be mediated by resveratrol: inhibition of tumor necrosis factor (TNF) α induced NFκB activity, cylcooxygenases (COX-1 and COX-2), aromatase, nitric oxide production in endotoxin-stimulated macrophages, proliferation of KB or MCF7 cells, induction of quinone reductase 1 (QR1), accumulation in the sub-G_1 phase of the cell cycle, and quenching of 2,2-diphenyl-1-picrylhydrazyl (DPPH) free radical. Two metabolites showed activity in these assays; the 3-sulfate exhibited QR1 induction, DPPH free radical scavenging, and COX-1 and COX-2 inhibitory activities and the 4′-sulfate inhibited NFκB induction, as well as COX-1 and COX-2 activities. Resveratrol and its 3′-sulfate and 4-sulfate inhibit NO production by NO scavenging and down-regulation of iNOS expression in RAW 264.7 cells. Resveratrol sulfates displayed low antiproliferative activity and negligible uptake in MCF7 cells.

Introduction

Resveratrol (**1**, 3,5,4′-trihydroxystilbene) is a naturally occurring phytoalexin produced by various plants in response to environmental stress or pathogenic attack. It is present in peanuts, mulberries, blueberries, and grapes[1−3] and possesses numerous biological activities that result in antioxidant,[4] anti-inflammatory,[5−7] anti-ischemic,[8−10] neuroprotective,[11,12] anti-aging,[13−15] antiobesity,[16] antiviral,[17] cardioprotective,[18−20] anticancer,[21] and cancer chemopreventive effects.[1,22−24] As a cancer chemopreventive agent, resveratrol has been shown to interfere with or inhibit all three stages of carcinogenesis: initiation, promotion, and progression.[1] Interestingly, it is apparent that resveratrol can elicit these effects even though serum concentrations are low.[25] Although resveratrol is efficiently absorbed on oral administration, rapid metabolism leads to the production of sulfates and glucuronides.[25−34] These facts cast doubt on the physiological relevance of the high resveratrol concentrations typically used for in vitro studies and suggest that at least some, if not most, of the biological effects elicited by resveratrol may be attributed to resveratrol metabolites.

Several resveratrol absorption and metabolism studies have been performed in rodent models. Initially, an isolated rat small intestine perfusion model was used.[29] Kuhnle and co-workers reported that orally administered resveratrol is mainly converted to glucuronide conjugates.[29] The metabolism of resveratrol was also investigated by Yu et al., who carried out oral and intraperitoneal injections with rats and mice.[31] Using synthetic standards, they identified *trans*-resveratrol-3-*O*-glucuronide and *trans*-resveratrol 3-sulfate in mouse serum.[31] Similar to previous findings, the glucuronide and sulfate conjugates of resveratrol were detected in rat urine and mouse serum, with minimal amounts of unchanged resveratrol.[31] Wenzel et al. established that all five possible resveratrol sulfate metabolites, as well as the 3-*O*-β-D-glucuronide, are produced in rats.[25]

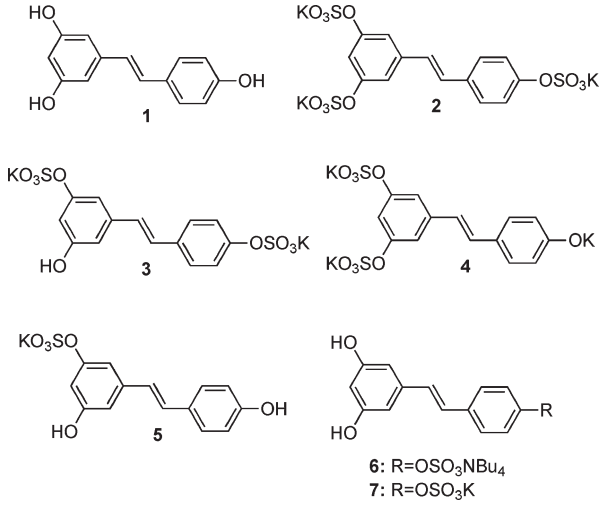

Resveratrol metabolism studies with human beings have produced results similar to those obtained with rodent models. De Santi et al. reported the sulfation and glucuronidation of resveratrol in human liver samples[26,27] and also observed sulfation in a human duodenum preparation.[28] Goldberg and collaborators demonstrated that after oral or iv injection, the majority of resveratrol detected in serum and urine was glucuronide and sulfate conjugates.[35] Following that study, comparable data were reported by Meng et al., who found that no more than 2.3% of the administered resveratrol is unchanged.[33] Walle et al. investigated the absorption, bioavailability, and metabolism of resveratrol by administering

*To whom correspondence should be addressed. Phone: 765-494-1465. Fax: 765-494-6790. E-mail: cushman@pharmacy.purdue.edu.

Published on Web 06/08/2010

Scheme 1[a]

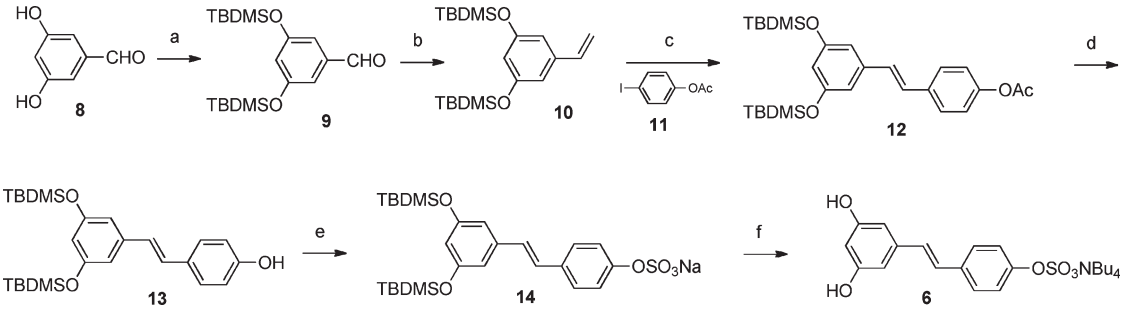

[a] Reagents and conditions: (a) TBDMSCl, DMF, 80%; (b) $NaNH_2$, $MePPh_3Br$, Et_2O, 72%; (c) $Pd(OAc)_2$, Et_3N, PPh_3, MeCN, 40%; (d) NaOMe, MeOH, 92%; (e) SO_3−pyridine, pyridine; (f) TBAF, MeOH, 15% (for steps e and f).

^{14}C-resveratrol to human subjects, confirming the findings that resveratrol is metabolized quickly and extensively.[34] All of these in vivo studies support the idea of resveratrol being predominantly converted to its glucuronic acid and sulfate conjugates after oral, ip, or iv administration.[25,29,32−36]

On the basis of resveratrol metabolism studies, it is reasonable to suggest that the in vitro data obtained using high concentrations of resveratrol lack direct in vivo relevance. Although administration of resveratrol has led to responses such as anticancer[21] and cancer chemopreventive[37−39] activities in animal models, it remains a fact that rapid and extensive metabolism leads to glucuronides and sulfates. Accordingly, response data could be explained by (1) local chemopreventive effects in the GI tract before metabolism occurs,[37,39] (2) the conversion of resveratrol sulfates and glucuronides back to resveratrol in target organs such as the liver,[25,32] (3) enterohepatic recirculation involving biliary secretion of resveratrol metabolites followed by deconjugation by gut microflora and then reabsorption,[36] and (4) the possible biological activities of the resveratrol metabolites themselves. The last has been suggested for other compounds, such as quercetin, (−)-epicatechin, and (+)-catechin.[40−42]

Selective chemical syntheses of glucuronide conjugates have been reported,[43,44] and syntheses of sulfated resveratrol are known as well. However, these are nonregioselective syntheses that requires HPLC separation of mono-, di-, and trisulfated conjugates.[25,45] As such, these procedures impede the preparation of sufficient quantities of sulfates required for a systematic investigation of their biological activities. In order to address this limitation, we have synthesized the previously identified resveratrol sulfate metabolites. All five metabolites have been prepared and isolated as their salts, and the biological effects of each metabolite have been investigated in a set of assays that are associated with cancer chemopreventive activity.

Results and Discussion

Chemistry. The synthesis of the five resveratrol sulfate metabolites is complicated by the fact that there are two different mono- and two different disulfated resveratrol compounds. This means that, regardless of the type of synthetic scheme that is utilized, there needs to be a way to selectively protect the three hydroxyl groups present in the resveratrol structure. Thus, the 4′-sulfate **6** was chosen as the first target because of the ease of selective protection of the 3,5-hydroxyl groups.

Compounds **10** and **11** were selected as the two reactants to undergo the Heck coupling. TBDMS[a] and acetate groups were chosen in order to increase the yield[46] and enable selective cleavage under different conditions (Scheme 1). As reported previously,[46] acetyl migrations have been observed during the Heck reaction; nevertheless, successful formation of compound **12** was confirmed. Following this, a catalytic amount of NaOMe was used to cleave the acetate group to generate **13**. The sulfation of **13** posed several problems. Since intermediate **14** is a sulfate sodium salt, it was not practical to perform organic extraction to remove inorganic impurities. It was therefore purified by applying the concentrated reaction mixture to a silica gel column, using EtOAc and MeOH as the solvent system. Deprotection of **14** with TBAF provided the tetra-*n*-butylammonium salt **6**.

The synthesis of **6** made it apparent that it is not easy to prepare and purify sulfated resveratrol metabolites. The published literature correctly states that the multiple sulfation reaction is "a synthetic nightmare".[47] For that reason the synthesis of trisulfated resveratrol **2** was attempted next in order to optimize the sulfation reaction, sulfate salt formation, and sulfate salt purification steps using commercially available resveratrol as the starting material (Scheme 2).

The first difficulty encountered in the process of synthesizing **2** was the method used to monitor the progress of the sulfation reaction. Switching the sulfation reagent from the $SO_3\cdot$pyridine complex to $SO_3\cdot NMe_3$ facilitated the TLC monitoring of the reaction and made the workup more convenient. Since trisulfated resveratrol is a very polar compound, the types of TLC plates used were changed from normal-phase to reversed-phase.

After driving the sulfation reaction to completion, the next challenge in the synthesis of trisulfated resveratrol metabolite **2** was forming the sulfate salts. Initial attempts using excess Na_2CO_3 made it clear that removal of inorganic salt from the product was very difficult because of the highly polar nature of the desired product. Use of a Dowex 50X8-200 column that had been converted to the K^+ form enabled formation of the tripotassium salt while limiting the introduction of excess K^+ into the reaction mixture. The final traces of inorganic impurities were removed by size exclusion chromatography.

The synthesis of mono- and disulfated resveratrol metabolites requires the preparation of four different precursors

[a] Abbreviations: COX-1, cyclooxygenase-1; COX-2, cyclooxygenase-2; DIPEA, diisopropylethylamine; DMSO, dimethyl sulfoxide; DMEM, Dulbecco's modified Eagle's medium; DPPH, 2,2-diphenyl-1-picrylhydrazyl; FTIR, Fourier transform infrared spectroscopy; LPS, lipopolysaccharide; QR1, quinone reductase-1; SNP, sodium nitroprusside; TBAF, tetra-*n*-butylammonium fluoride; TBDMS, *tert*-butyldimethylsilyl; TBDMSCl, *tert*-butyldimethylsilyl chloride; TNF-α, tumor necrosis factor α.

Scheme 2[a]

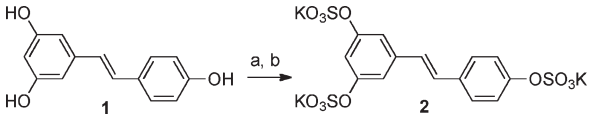

[a] Reagents and conditions: (a) SO_3−NMe_3, MeCN, Et_3N, reflux, 21%; (b) Dowex 50WX8-200 ion exchange column, K^+ form.

Scheme 3[a]

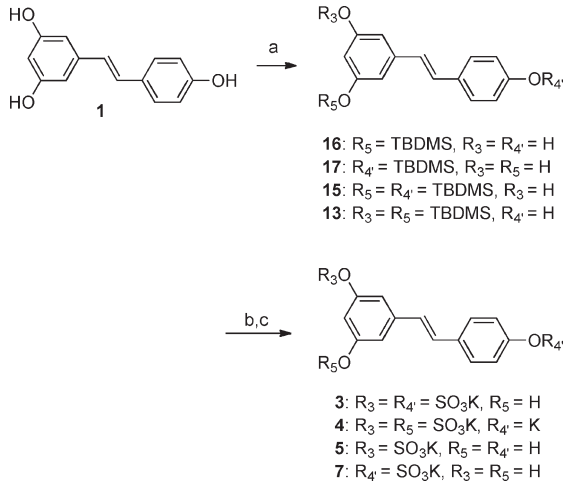

[a] Reagents and conditions: (a) TBDMSCl, imidazole, DMF, 12−33%; (b) SO_3−NMe_3, MeCN, Et_3N; (c) KF, MeOH/H_2O, 15−26% (for steps b and c).

(Scheme 3). These precursors require selective protection of three hydroxyl groups that are present on the stilbene framework. The protected intermediates necessary to synthesize mono- and disulfated resveratrol were prepared and separated (Scheme 3, compounds **13**, **15**−**17**) following the procedure established by Zhang et al.[43] By use of the previously determined reaction conditions, each of the four TBDMS-protected resveratrol compounds was sulfated. At this point, these sulfated intermediates were not converted to potassium sulfates because of observation that not forming potassium salts before the deprotection step enhanced the solubilities of the intermediate with both nonpolar TBDMS groups and polar sulfate groups. Although the difference appears minimal, not forming potassium salts greatly improved the solubilities of the intermediates and made it possible to effectively remove organic impurities from the reaction mixture before the TBDMS deprotection reaction. The TBDMS deprotection reactions were carried out with KF instead of TBAF in order to avoid formation of the tetra-*n*-butylammonium salts. By combination of these optimization efforts, four different potassium salts **3**−**5** and **7** of sulfated resveratrol metabolites were successfully formed, as shown in Scheme 3.

The NMR peak assignments for all possible sulfated resveratrol metabolites are compared in Table 1. As expected, the signals move downfield as sulfates are added. The ^1H NMR chemical shifts and coupling constants, along with the mass spectrometry data, allowed the unambiguous assignments of the structures of all five metabolites. In particular, the equivalence or nonequivalence of the protons attached to C-2 and C-6 was diagnostic.

Biological Results. One of the most extensively studied biological activities of resveratrol investigated during the past few years has been its cancer-chemopreventive potential.[48] This stilbene has been demonstrated to block the multistep process of carcinogenesis at the various stages of initiation, promotion, and progression. Some possible mechanisms involve down-regulation of the inflammatory response through inhibition of synthesis and release of pro-inflammatory mediators, modification of eicosanoid synthesis, inhibition of activated immune cells, or inhibition of inducible nitric oxide synthase (iNOS) and cyclooxygenase-2 (COX-2) via modulation of NFκB. To explore the activities of the synthetic resveratrol sulfate derivatives, they were tested in a set of assays indicative of chemoprevention, including inhibition of TNF-α-induced NFκB activity, COX-1 and COX-2 inhibition, inhibition of nitric oxide production by iNOS in LPS-induced macrophage cells, aromatase inhibition, QR1 induction, 2,2-diphenyl-1-picrylhydrazyl (DPPH) free radical quenching, and cytotoxicity in KB and MCF7 cells. The results are summarized in Table 2.

Table 1. ^1H NMR (in D_2O) Shifts (ppm) for Sulfated Resveratrols

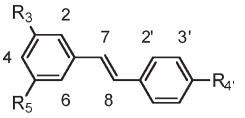

	proton assignment						
compd	4	2	6	7	8	2′	3′
resveratrol	5.41	5.68	5.68	6.60	6.33	6.94	6.20
2	7.03	7.26	7.26	7.14	7.03	7.49	7.15
3	6.38	6.65	6.71	7.05	6.94	7.46	7.14
4	6.94	7.18	7.18	7.01	6.83	7.31	6.70
5	6.54	6.77	6.88	7.02	6.84	7.34	6.74
6	not soluble in D_2O						
7	6.13	6.47	6.47	6.97	6.84	7.40	7.11

The role of NFκB in many cellular processes is well studied. Deregulated activity of the NFκB pathway has been observed and linked to the progression of cancer and several human ailments. Our test system assesses inhibition of NFκB induction by TNF-α in a stably transfected 293/NFκB-Luc human embryonic kidney cell line.[49] Presumably, the sulfate metabolites could be transported intact into the kidney cells by organic anion transporters.[50−53]All of the metabolites retained some level of activity in this assay, but potency was reduced, relative to resveratrol. The most active metabolite was the 4′-sulfate **7**, and the two least active were **2** and **4**. In general, the ability of these stilbenes to inhibit the induction of NFκB is surprisingly insensitive to the substituents present or to their arrangement.

The involvement of prostaglandins (PG) and other eicosanoids in the development of human cancer is well-known.[54] Importantly, an increase in PG synthesis may influence tumor growth in human beings and experimental animals. Cleaved from membrane phospholipids by phospholipases, arachidonic acid (AA) is converted through the cyclooxygenase (COX) pathway to produce PGs.[55] Therefore, inhibition of COX and the subsequent reduction of PG synthesis provides a viable strategy for the prevention of cancer.[56−60] Accordingly, resveratrol and resveratrol sulfates were tested for inhibition of both COX-1 and COX-2. Resveratrol inhibited COX-1 and -2 with IC_{50} values of 6.65 and 0.75 μM, respectively. The 3-sulfate **5** and the 4′-sulfate **7** inhibited COX-1 with IC_{50} values comparable to resveratrol (3.60 and 5.55 μM, respectively). In COX-2 inhibition assays,

Table 2. Biological Evaluation of Resveratrol and Resveratrol Sulfates in Bioassays Indicative of Cancer Chemoprevention

	compounds tested					
assay	resveratrol	**2**	**3**	**4**	**5**	**7**
NFκB						
% inhibition[a]	75.7 ± 2.12	36.7 ± 9.4	53.4 ± 2.9	42.5 ± 5.23	33.0 ± 4.81	64.0 ± 2.26
IC_{50} (μM)	0.173 ± 0.05					18.2 ± 0.99
COX-1						
% inhibition[a]	75.2 ± 4.53	37.8 ± 0.71	23.3 ± 0.98	30.9 ± 2.69	74.3 ± 0.99	63.2 ± 3.39
IC_{50} (μM)	6.65 ± 2.5				3.60 ± 0.8	5.55 ± 1.73
COX-2						
% inhibition[a]	72.2 ± 4.67	2.4 ± 2.0	16.5 ± 2.69	25.5 ± 5.52	62.0 ± 1.7	65.8 ± 7.64
IC_{50} (μM)	0.75 ± 0.52				7.53 ± 4.7	8.95 ± 1.2
nitric oxide production						
% inhibition[a]	71.8 ± 3.5	24.8 ± 3.1	41.7 ± 5.5	4.8 ± 4.5	41.0 ± 0.7	56.8 ± 5.9
IC_{50} (μM)	15.0 ± 2.6					
% sub-G_1[a,b]	24.9 ± 0.149					2.22 ± 0.012
cytotoxicity[c]						
KB % survival	47.8 ± 5.2	78.1 ± 7.8	99.3 ± 15.0	84.2 ± 13.1	70.3 ± 8.8	108.5 ± 10.3
MCF7% survival	38.6 ± 3.5	106.7 ± 9.6	100.0 ± 11.3	97.2 ± 5.2	51.7 ± 0.2	103.4 ± 8.8
aromatase						
% inhibition[a]	34.8 ± 1.21	28.5 ± 0.2	22.5 ± 0.64	20.5 ± 0.43	28.2 ± 1.12	30.4 ± 0.56
QR1						
CD (μM)[d]	21 ± 0.46	> 11.7	> 10.1	> 10.1	2.6 ± 0.38	> 6.9
DPPH						
% inhibition[e]	65.2 ± 2.0	0.4 ± 1.1	6.8 ± 1.0	14.5 ± 4.2	68.0 ± 1.9	42.8 ± 2.5
IC_{50} (μM)	178.5 ± 9.3				219.2 ± 3.1	

[a] Determined at a compound concentration of 34 μM. The compounds were not cytotoxic at this concentration in HEK-293 cells. [b] The percentage of subG$_1$ HL-60 cells, characteristic of apoptosis. The distribution in sub-G_1 of vehicle-treated cells was 2.2 ± 0.0%. [c] Determined at 20 μg/mL. [d] Concentration to double the expression of QR1. [e] Determined at a compound concentration of 340 μM.

the 3-sulfate **5** demonstrated an IC_{50} of 7.53 μM and the 4′-sulfate **7** had an IC_{50} of 8.95 μM.

Nitric oxide (NO), a product of nitric oxide synthase (NOS), mediates diverse physiological processes (e.g., vasodilation, immune response) as a signaling molecule. However, continuous and excessive production of NO by inducible nitric oxide synthase (iNOS) causes pathophysiological problems such as chronic inflammatory diseases and cancer development.[61] In addition, up-regulation of nitric oxide (NO) synthesis may contribute to tumor growth by facilitating angiogenesis.[62] Inhibitors of inducible nitric oxide synthase (iNOS) may have chemopreventive activity due to antiproliferative effects,[56] and resveratrol has been reported to function in this capacity.[63] Therefore, the abilities of resveratrol and resveratrol sulfates to inhibit the production of NO by iNOS in macrophage cells were determined. With an IC_{50} value of 15 μM, resveratrol was the most potent inhibitor of nitric oxide synthase. Modest activity was observed with 4′-sulfate **7**, followed by the 3,4′-disulfate **3** and the 3-sulfate **5**, which were equipotent. The least potent nitric oxide synthase inhibitor was the 3,5-disulfate **4**, which was actually less potent than the trisulfate **2**.

To determine whether resveratrol sulfates induce nitric oxide production by themselves, these compounds were tested under LPS-free circumstances. None of the resveratrol sulfates showed significant enhancement of NO production when tested at 34 μM (data not shown).

Several publications have indicated that polyphenols like resveratrol[64] and epigallocatechin gallate (EGCG)[65] inhibit NO and peroxynitrite formation because of antioxidant activity.[66] Therefore, NO scavenging activity of each resveratrol sulfate was measured using the NO generating reagent sodium nitroprusside (SNP). At 60 μM, compounds **1**, **5**, and **7** showed slight NO scavenging activity, with 17.4 ± 4.3%, 24.7 ± 1.2%, 10.3 ± 4.3% inhibition, while compounds **2**, **3**, and **4** were not active, demonstrating 1.6 ± 3.8%, 0.0 ± 3.3%, and 1.2 ± 4.9% inhibition, respectively

Several polyphenols, including 6-gingerol, epigallocatechin gallate (EGCG), indole-3-carbinol, and oroxylin A, as well as resveratrol itself, have been reported to inhibit iNOS expression in LPS-treated RAW 264.7 cell lines.[67] We performed Western blot analyses to determine if compounds **1**, **5**, **7** inhibit nitrite production via down-regulation of iNOS expression. As shown in Figure 1, LPS increased the protein expression of iNOS in comparison with untreated RAW 264.7 cells. Under the same conditions, resveratrol sulfates **1**, **5**, **7** moderately suppressed the expression of iNOS compared to LPS-treated control. In sum, compounds **1**, **5**, **7** showed moderate inhibition in NO production by NO scavenging activity and down-regulation of iNOS protein expression. Although these responses are not strong, since up-regulation of iNOS is correlated with activation of upstream NFκB pathways[61] and some inhibitors of NO production function through NFκB regulation,[68] a compound such as **7** could possibly mediate a stronger response in a broader biological milieu.

Using the same experimental approach simultaneously, we investigated protein expression of COX-2 (Figure 1). None of tested compounds at 34 μM inhibited COX-2 expression, which is consistent with a previous report.[69]

Resveratrol is known to induce programmed cell death (apoptosis) in a variety of cell lines, including lung, colon, prostate, and breast.[70−73] Since a sub-G_1 cell population is an indicator of cell death by apoptosis or necrosis, we explored the potential of resveratrol and resveratrol sulfates to induce accumulation of HL-60 human acute leukemia cells in the sub-G_1 compartment. Consistent with previous results,[74] resveratrol was active in this process, but the sulfate metabolites were inactive.

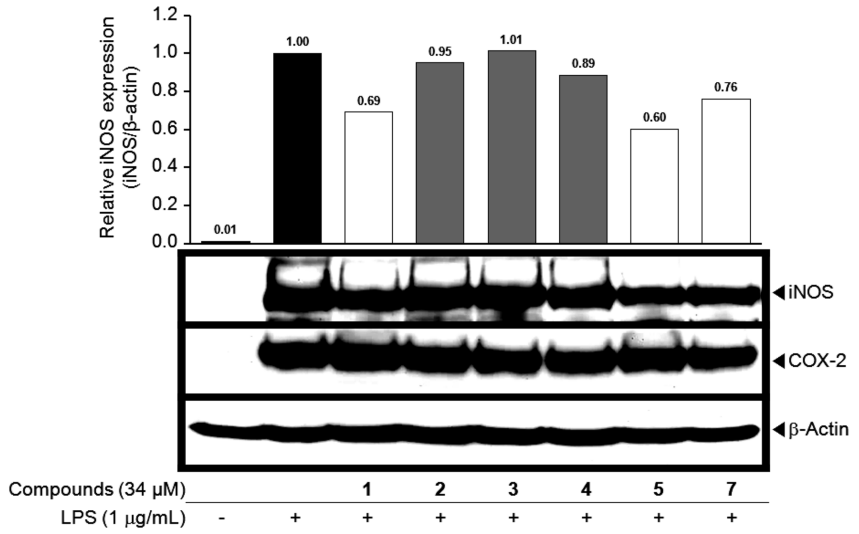

Figure 1. Effects of resveratrol and its sulfate derivatives on iNOS and COX-2 expression in LPS-stimulated RAW 264.7 cells. RAW 264.7 cells were treated with compounds 15 min prior to LPS (1 μg/mL) stimulation and further incubated for 18 h. Cells were lysed, and protein (30 μg) was subjected to 8% SDS−PAGE. The level of iNOS and COX-2 protein expression was examined by immunoblot analysis. β-Actin was used as an internal control. The experiment was performed in duplicate. The density of each band was measured by using an image analyzer system. Average values of relative iNOS protein expression are shown in comparison with the LPS-treated control (black bar). Compounds **1**, **5**, and **7** (open bars) showed suppressive effects on the expression of iNOS protein with relative values of 0.69, 0.60, and 0.76, respectively. Compounds **2**, **3**, and **4** were not active, and COX-2 expression was not altered.

The lack of cytotoxicity of the sulfates **2**−**4** and **7** in MCF7 and KB cells (Table 2), as well as low activity in other cell-based assays, suggests a lack of uptake as well as a lack of hydrolysis. To test for cellular uptake, the 3,5-disulfate **4** and resveratrol were incubated separately with MCF7 cells, and LC−MS−MS was used to measure intracellular levels of resveratrol and its various sulfate conjugates. After incubation with resveratrol as a control, MCF7 cells were found to contain resveratrol and the disulfate **4** but not the 4′-sulfate **7**. This indicated that resveratrol entered MCF7 cells and was metabolized to form **7**. When MCF7 cells were incubated with the 4′-sulfate **7**, no absorption of **7** was detected, and neither resveratrol **1** nor the disulfate **4** was detected intracellularly. These results indicate lack of hydrolysis and uptake of the 4′-sulfate **7** by MCF7 cells. On the basis of the cytotoxicity results (Table 2), the other sulfates are probably also not hydrolyzed or absorbed to an appreciable extent by MCF7 cells.

To test the stability of resveratrol and its 4′-sulfate **7**, each compound was incubated separately for 24 h at 37 °C in the cell culture medium used for MCF7 cellular uptake studies. On the basis of LC−MS−MS analyses, the 4′-sulfate **7** was stable under these incubation conditions. On the other hand, resveratrol **1** degraded approximately 20% during this time period. Therefore, metabolic sulfation of resveratrol forms stable derivatives that can be excreted in bile or urine. Since enterohepatic recirculation of resveratrol occurs,[36] resveratrol sulfates will be deconjugated by gut microflora, and then resveratrol will be reabsorbed to prolong its anticancer effects.

CYP19 (aromatase) converts C19 androgens to aromatic C18 estrogens through three consecutive hydroxylation reaction steps.[75] Aromatase transcription is mediated by IκB kinase β (IKKβ), a kinase previously known for cancer-promoting activity.[76] Under some situations (e.g., postmenopause), aromatase is a key player in estrogen production, and inhibitors have been shown to function as chemopreventive agents. On the basis of an in vitro test system, resveratrol and its sulfates were found to be relatively weak inhibitors. The most active of the metabolites was the 4′-sulfate **7**, which produced 30% inhibition at 34 μM.

Induction of NAD(P)H/quinone reductase 1 (QR1) is a well established mechanism for cancer chemoprevention.[77−80] Induction of QR1 commonly coincides with the induction of other phase II detoxifying enzymes.[81] Therefore, a rapid and sensitive QR1 cellular assay[82] was used to evaluate resveratrol and resveratrol metabolites. In addition, the concentrations to double the activity of QR1 (CD) are listed. The 3-sulfate **5** was more potent than resveratrol in this assay, while the other sulfate metabolites were all less potent. However, all of the sulfates retained some degree of activity.

The cancer chemopreventive effects of resveratrol and related phenolic natural products may be due, in part, to quenching unstable free radicals and reducing damage to DNA by reactive oxygen species (ROS).[83−85] The free-radical scavenging activities of the test compounds were examined by measuring the ability to quench the DPPH radical. The activity of the 3-sulfate **5** was comparable to that of the parent compound **1**, while the activity of the 4′-sulfate **7** was somewhat lower. The remaining disulfates **3** and **4** were much less active as free radical scavengers, and as expected from the absence of any phenolic hydroxyl groups, the trisulfate **2** was inactive.

Conclusion

Resveratrol exerts chemopreventive activity, and a host of targets have been established.[86] We selected a variety of in vitro and cell-based targets (Table 2) to determine the activity displayed by resveratrol relative to sulfate metabolites. Overall, the sulfate metabolites are less active than resveratrol, with some exceptions, such as resveratrol 3-sulfate (**5**), which mediates comparable or even greater QR1 induction, DPPH radical scavenging, and COX-1 inhibition. Not surprisingly, in general, the activities of the sulfate metabolites decrease as the degree of sulfation increases, although there are exceptions (e.g., the activities of **2** vs **4** on inhibition of nitric oxide

synthase). Since serum concentrations of sulfated metabolites are higher than the serum concentrations of resveratrol, the ability of the metabolites to typically retain some degree of activity may be of relevance.

Experimental Section

Melting points were determined using capillary tubes with a Mel-Temp apparatus and are uncorrected. The proton nuclear magnetic resonance spectra were recorded using an ARX300 300 MHz Bruker NMR spectrometer. IR spectra were recorded using a Perkin-Elmer 1600 series FTIR spectrometer. Flash and gravity chromatographic purification were performed using 230−400 mesh silica gel unless otherwise noted. Chemicals and solvents were reagent grade and obtained from commercial sources without further purification. Synthetic compounds were analyzed at the Purdue University Campus-Wide Mass Spectrometry Center using a Finnigan MAT LCQ Classic mass spectrometer system equipped with electrospray. Combustion microanalyses were performed at the Purdue University Microanalysis Laboratory using a Perkin-Elmer series II CHNS/O model 2400 analyzer, and all reported values are within 0.4% of calculated values. These elemental analyses confirmed ≥95% purity.

Resveratrol Tripotassium 3,5,4′-Sulfate (2). A mixture of $SO_3 \cdot NMe_3$ (1.097 g, 7.886 mmol) in Et_3N (2.50 mL, 13.14 mmol) was added to a well-stirred mixture of **1** (0.100 g, 0.438 mmol) in anhydrous MeCN (5.0 mL) at room temperature under argon. The resulting reaction mixture was heated at reflux under argon for 120 h. The reaction mixture was cooled to room temperature, decanted, and concentrated under reduced pressure. Water (5.0 mL) was added to the reaction mixture, and the resulting mixture was stirred for 30 min at room temperature. The water layer was concentrated to approximately 2.0 mL and applied to a column of cation-exchange resin (Dowex 50WX8-200, H^+ form, 9 g, 2 cm × 19 cm) prepared by eluting solvents in the following order: water (300 mL), saturated K_2CO_3 solution (400 mL), and water (300 mL). The crude product was eluted with water, and fractions containing the desired intermediate were combined and concentrated and applied to a column of reversed-phase C-18 silica gel (eluent 0−20% MeOH−H_2O, reversed-phase C-18 silica gel, 6 g, 2 cm × 11 cm). Fractions containing the desired compound were combined and concentrated. The crude product was applied to a size-exclusion chromatography column (eluent H_2O, Sephadex G-10, 14 g, 2 cm × 20 cm) to afford **2** as a white solid (0.054 g, 21%): mp > 350 °C. ^{1}H NMR (300 MHz, D_2O) δ 7.49 (d, J = 8.7 Hz, 2 H), 7.26 (d, J = 2.1 Hz, 2 H), 7.15 (d, J = 8.7 Hz, 2 H), 7.14 (d, J = 16.5 Hz, 1 H), 7.03 (d, J = 16.5 Hz, 1 H), 6.99 (t, J = 2.1 Hz, 1 H); positive ESIMS m/z (rel intensity) 621 (MK^+, 100). Anal. Calcd for $C_{14}H_9K_3O_{12}S_3 \cdot 1.25H_2O$: C, 27.78; H, 1.92; S, 15.89. Found: C 27.54; H, 1.77; S, 15.62.

Resveratrol Dipotassium 3,4′-Sulfate (3). $SO_3 \cdot NMe_3$ (0.487 g, 3.504 mmol) and Et_3N (0.81 mL, 5.83 mmol) were added to a well-stirred mixture of **16** (0.100 g, 0.292 mmol) in anhydrous MeCN (5.0 mL) at room temperature under argon. The resulting reaction mixture was heated to reflux under argon for 48 h. The reaction mixture was cooled to room temperature, decanted, concentrated under reduced pressure, and applied to a column of reversed-phase C-18 silica gel (eluent 10−25% CH_3CN−H_2O, 5 g, 2 cm × 10 cm). Fractions containing the desired compound and some impurities were combined, concentrated, and dissolved in 30% aqueous MeOH (10 mL). KF (0.051 g, 0.875 mmol) was added to the solution, which was stirred vigorously at room temperature under argon for 12 h and concentrated under reduced pressure. The crude product was applied to a column of cation-exchange resin (Dowex 50WX8-200, H^+ form, 9 g, 2 cm × 19 cm) prepared by eluting solvents in the following order: water (300 mL), saturated K_2CO_3 solution (400 mL), and water (300 mL). The crude product was eluted with water, and fractions containing the desired intermediate were combined, concentrated, and applied to a column of reversed-phase C-18 silica gel (eluent 0−20% MeOH−H_2O, 6 g, 2 cm × 11 cm). Fractions containing the desired compound and some impurities were combined, concentrated, and applied to a size-exclusion chromatography column (eluent H_2O, Sephadex G-10, 14 g, 2 cm × 20 cm) to afford **3** as a white solid (0.015 g, 26%): mp > 300 °C. ^{1}H NMR (300 MHz, D_2O) δ 7.46 (d, J = 8.4 Hz, 2 H), 7.13 (d, J = 8.1 Hz, 2 H), 7.05 (d, J = 16.5 Hz, 1 H), 6.94 (d, J = 16.5 Hz, 1 H), 6.71 (s, 1 H), 6.65 (s, 1 H), 6.38 (t, J = 2.1 Hz, 1 H); positive ESIMS m/z (rel intensity) 487 (MNa^+, 100). Anal. Calcd for $C_{14}H_{10}K_2O_9S_2 \cdot 2H_2O$: C, 33.59; H, 2.82; S, 12.81. Found: C, 33.42; H, 2.38; S, 12.83.

Resveratrol Tripotassium 3,5-Sulfate (4). $SO_3 \cdot NMe_3$ (0.487 g, 3.504 mmol) and Et_3N (0.81 mL, 5.83 mmol) were added to a well-stirred mixture of **17** (0.100 g, 0.292 mmol) in anhydrous MeCN (5.0 mL) at room temperature under argon. The resulting reaction mixture was heated to reflux under argon for 48 h. The reaction mixture was cooled to room temperature, decanted, concentrated under reduced pressure, and applied to a column of reversed-phase C-18 silica gel (eluent 10−25% CH_3CN-H_2O, 5 g, 2 cm × 10 cm). Fractions containing the desired compound and some impurities were combined and concentrated and dissolved in 30% aqueous MeOH (10 mL). KF (0.051 g, 0.875 mmol) was added to the solution, which was stirred vigorously at room temperature under argon for 12 h and concentrated under reduced pressure. The crude product was applied to a column of cation-exchange resin (Dowex 50WX8-200, H^+ form, 9 g, 2 cm × 19 cm) prepared by eluting solvents in the following order: water (300 mL), saturated K_2CO_3 solution (400 mL), and water (300 mL). The crude product was eluted with water, and fractions containing the desired intermediate and some impurities were combined and concentrated and applied to a column of reversed-phase C-18 silica gel (eluent 0−20% MeOH−H_2O, 6 g, 2 cm × 11 cm). Fractions containing the desired compound and some impurities were combined and concentrated and applied to a size-exclusion chromatography column (eluent H_2O, Sephadex G-10, 14 g, 2 cm × 20 cm) to afford **4** as a white solid (0.015 g, 20%): mp > 300 °C. ^{1}H NMR (300 MHz, D_2O) δ 7.31 (d, J = 8.7 Hz, 2 H), 7.18 (d, J = 2.1 Hz, 2 H), 7.01 (d, J = 16.2 Hz, 1 H), 6.94 (t, J = 2.1 Hz, 1 H), 6.83 (d, J = 16.5 Hz, 1 H), 6.70 (d, J = 8.7 Hz, 2 H); positive ESIMS m/z (rel intensity) 487 (MNa^+, 100). Anal. Calcd for $C_{14}H_9K_3O_9S_2 \cdot 2H_2O$: C, 31.22; H, 2.43; S, 11.91. Found: C, 30.94; H, 2.26; S, 11.73.

Resveratrol Potassium 3-Sulfate (5). $SO_3 \cdot NMe_3$ (0.548 g, 3.948 mmol) and Et_3N (0.92 mL, 6.56 mmol) were added to a well-stirred mixture of **15** (0.300 g, 0.656 mmol) in anhydrous MeCN (5.0 mL) at room temperature under argon. The resulting reaction mixture was heated to reflux under argon for 48 h. The reaction mixture was cooled to room temperature, decanted, concentrated under reduced pressure, and applied to a column of reversed-phase C-18 silica gel (eluent 10−30% CH_3CN−H_2O, 5 g, 2 cm × 10 cm). Fractions containing the desired compound and some impurities were combined and concentrated and dissolved in anhydrous MeOH (10 mL). KF (0.051 g, 0.875 mmol) was added to the solution, which was stirred vigorously under argon at room temperature for 12 h and concentrated under reduced pressure. The resulting crude reaction mixture was applied to a column of cation-exchange resin (Dowex 50WX8-200, H^+ form, 8 g, 2 cm × 18 cm) prepared by eluting solvents in the following order: water (300 mL), saturated K_2CO_3 solution (400 mL), and water (300 mL). The crude product was eluted with water, and fractions containing the desired intermediate and some impurities were combined and concentrated and applied to a column of reversed-phase C-18 silica gel (eluent 0−30% MeOH−H_2O, 6 g, 2 cm × 11 cm). Fractions containing the desired compound and some impurities were combined and concentrated and applied to a size-exclusion chromatography column (eluent H_2O, Sephadex G-10, 14 g, 2 cm × 20 cm) to give **5** as a white solid (0.010 g, 15%): mp > 300 °C. ^{1}H NMR (300 MHz, D_2O) δ 7.34 (d, J = 8.7 Hz, 2 H), 7.02 (d,

J = 16.5 Hz, 1 H), 6.88 (s, 1 H), 6.84 (d, J = 16.5 Hz, 1 H), 6.77 (s, 1 H), 6.74 (d, J = 8.4 Hz, 2 H), 6.54 (t, J = 2.1 Hz, 1 H); positive ESIMS m/z (rel intensity) 386 (MK^+, 100). Anal. Calcd for $C_{14}H_{11}KO_6S$: C, 48.54; H, 3.20; S, 9.26. Found: C, 48.24; H, 3.12; S, 8.90.

Resveratrol Tetrabutylammonium 4′-Sulfate (6). TBAF (0.53 mL, 2.189 mmol) was added to a well-stirred mixture of **14** (0.100 g, 0.178 mmol) in MeOH (5.0 mL) at room temperature under argon. The resulting reaction mixture was stirred at room temperature under argon for 12 h. The reaction mixture was concentrated under reduced pressure, and the crude product was purified by recrystallization from methanol to afford the product **6** as a white solid (0.015 g, 15%): mp 182−184 °C. ^{1}H NMR (300 MHz, MeOH-d_4) δ 7.38 (d, J = 8.7 Hz, 2 H), 7.17 (d, J = 8.4 Hz, 2 H), 6.92 (d, J = 16.5 Hz, 1 H), 6.81 (d, J = 16.2 Hz, 1 H), 6.37 (d, J = 2.1 Hz, 2 H), 6.07 (t, J = 2.1 Hz, 1 H), 3.11 (t, J = 8.4 Hz, 8 H), 1.59−1.49 (m, 8 H), 1.36−1.23 (m, 8 H), 0.90 (t, J = 7.3 Hz, 12 H); positive ESIMS m/z (rel intensity) 353 (MNa^+, 100). Anal. Calcd for $C_{30}H_{47}NO_6S$: C, 65.54; H, 8.62; N, 2.55; S, 5.83. Found: C, 65.47; H, 8.63; N, 2.44; S, 5.74.

Resveratrol Potassium 4′-Sulfate (7). $SO_3 \cdot NMe_3$ (0.533 g, 3.829 mmol) and Et_3N (0.73 mL, 5.22 mmol) were added to a well-stirred mixture of **13** (0.330 g, 0.722 mmol) in anhydrous MeCN (8.0 mL) at room temperature under argon. The resulting reaction mixture was heated to reflux under argon for 48 h. The reaction mixture was cooled to room temperature, decanted, concentrated under reduced pressure, and applied to a column of reversed-phase C-18 silica gel (eluent 10−30% CH_3CN-H_2O, 5 g, 2 cm × 10 cm). Fractions containing the desired compound and some impurities were combined and concentrated and dissolved in anhydrous MeOH (10 mL). KF (0.054 g, 0.935 mmol) was added to the solution, which was stirred vigorously under argon at room temperature for 12 h and concentrated under reduced pressure. The resulting crude reaction mixture was applied to a column of cation-exchange resin (Dowex 50WX8-200, H^+ form, 8 g, 2 cm × 18 cm) prepared by eluting solvents in the following order: water (300 mL), saturated K_2CO_3 solution (400 mL), and water (300 mL). The crude product was eluted with water, and fractions containing the desired intermediate and some impurities were combined, concentrated, and applied to a column of reversed-phase C-18 silica gel (eluent 0−30% MeOH−H_2O, 6 g, 2 cm × 11 cm). Fractions containing the desired compound and some impurities were combined and concentrated and applied to a size-exclusion chromatography column (eluent H_2O, Sephadex G-10, 14 g, 2 cm × 20 cm) to give **7** as a light-brown solid (0.025 g, 10%): mp > 300 °C. ^{1}H NMR (300 MHz, D_2O) δ 7.40 (d, J = 8.4 Hz, 2 H), 7.11 (d, J = 8.4 Hz, 1 H), 6.97 (d, J = 16.5 Hz, 1 H), 6.84 (d, J = 16.5 Hz, 2 H), 6.47 (d, J = 2.1 Hz, 2 H), 6.13 (t, J = 2.1 Hz, 1 H); negative ESIMS m/z (rel intensity) 307 (100). Anal. Calcd for $C_{14}H_{11}KO_6S$: C, 48.54; H, 3.20; S, 9.26. Found: C, 48.19; H, 3.05; S, 8.95.

3,5-Bis(*tert*-butyldimethylsilyloxy)benzaldehyde (9). TBDMSCl (2.73 g, 14.5 mmol) was added to **8** (1.00 g, 7.24 mmol) in DMF (10 mL) at 0 °C under argon. The reaction mixture was stirred for 16 h at room temperature. Water (50 mL) was added to the reaction mixture, and the mixture was extracted with CH_2Cl_2 (3 × 100 mL). The combined organic layers were dried over sodium sulfate and concentrated. The resulting crude product was purified by column chromatography (eluent hexanes−EtOAc, 9:1, silica gel) to afford the product **9** as an orange oil (2.12 g, 80%). IR (film) 3072, 2956, 2931, 2886, 1704, 1384, 1259, 1031 cm^{-1}; ^{1}H NMR (300 MHz, $CDCl_3$) δ 9.86 (s, 1 H), 6.95 (d, J = 2.1 Hz, 1 H), 6.58 (t, J = 2.1 Hz, 1 H), 0.98 (s, 18 H), 0.21 (s, 12 H); ^{13}C NMR (75 MHz, $CDCl_3$) δ 191.6, 157.6, 138.8, 118.6, 114.6, 25.9, 18.5, −4.1; EIMS m/z (rel intensity) 366 (M^+, 100), 309 (96), 267 (58), 239 (52), 84 (78), 73 (70). Anal. Calcd for $C_{19}H_{34}O_3Si_2$: C, 62.24; H, 9.41. Found: C, 61.90; H, 9.41.

(5-Vinyl-1,3-phenylene)bis(oxy)bis(*tert*-butyldimethylsilane) (10). A reaction mixture containing $MePPh_3Br$ (2.93 g, 8.20 mmol), $NaNH_2$ (0.319 g, 8.20 mmol), and dry ether (12.0 mL) was stirred under argon at room temperature for 20 h. The reaction mixture was cannulated into a well-stirred mixture of **9** (0.300 g, 0.820 mmol) in dry ether (1.0 mL) at −10 °C under argon. After 10 min, the ice bath was removed and the reaction mixture was stirred at room temperature for 5 h. The crude product was concentrated and purified by column chromatography (eluent hexanes, silica gel) to provide the product **10** as a clear oil (0.21 g, 72%). IR (film) 3056, 2930, 1584, 1471, 1255, 1061 cm^{-1}; ^{1}H NMR (300 MHz, $CDCl_3$) δ 6.60 (dd, J = 17.8, 10.8 Hz, 1 H), 6.55 (d, J = 2.1 Hz, 2 H), 6.28 (t, J = 2.4 Hz, 1 H), 5.68 (dd, J = 17.8, 0.9 Hz, 1 H), 5.22 (dd, J = 10.8, 0.9 Hz, 1 H), 1.00 (s, 18 H), 0.24 (s, 12 H); ^{13}C NMR (75 MHz, $CDCl_3$) δ 157.0, 139.8, 137.2, 114.3, 112.1, 111.9, 26.1, 18.7, −3.9; positive ESIMS m/z (rel intensity) 365 (MH^+, 100). Anal. Calcd for $C_{20}H_{36}O_2Si_2$: C, 65.87; H, 9.95; Si, 15.40. Found: C, 65.48; H, 9.65, Si, 15.53.

4-Iodophenyl Acetate (11). Ac_2O (3.44 mL, 36.36 mmol) was added to a well-stirred mixture of 4-iodophenol (4.00 g, 18.18 mmol) in dry pyridine (15 mL) at room temperature under argon. The resulting reaction mixture was stirred at room temperature under argon for 12 h. H_2O (40 mL) was added, and the mixture was extracted with $CHCl_3$ (3 × 40 mL). The combined organic layers were washed with citric acid (10% w/v) to remove extra pyridine. The resulting crude product was purified by column chromatography (eluent $CHCl_3$, silica gel) to provide the product as a clear oil (0.823 g, 53%). ^{1}H NMR (300 MHz, $CDCl_3$) δ 7.66 (d, J = 8.4 Hz, 2 H), 6.84 (d, J = 8.7 Hz, 2 H), 2.26 (s, 3 H); EIMS m/z (rel intensity) 262 (M^+, 23), 220 (100).

(*E*)-4-(3,5-Bis(*tert*-butyldimethylsilyloxy)styryl)phenyl Acetate (12).[46] Et_3N (1.25 mL), $Pd(OAc)_2$ (0.008 g, 0.038 mmol), and PPh_3 (0.006 g, 0.025 mmol) were added to a well-stirred mixture of **10** (1.865 g, 5.114 mmol), **11** (1.00 g, 3.816 mmol), and CH_3CN (10 mL) at room temperature under argon. The reaction mixture was heated to reflux under argon for 35 h. The resulting suspension was extracted with Et_2O (3 × 30 mL). The combined organic layers were washed with water (1 × 20 mL) and brine (1 × 20 mL), dried over sodium sulfate, and concentrated to provide the product **12** as a clear oil (0.760 g, 40%). ^{1}H NMR (300 MHz, $CDCl_3$) δ 7.32 (d, J = 8.7 Hz, 2 H), 6.90 (d, J = 8.4 Hz, 2 H), 6.82 (d, J = 16.5 Hz, 1 H), 6.74 (d, J = 16.5 Hz, 1 H), 6.45 (d, J = 2.1 Hz, 2 H), 6.10 (t, J = 2.1 Hz, 1 H), 2.11 (s, 3 H), 0.81 (s, 18 H), 0.06 (s, 12 H); ^{13}C NMR (75 MHz, $CDCl_3$) δ 169.9, 157.2, 150.5, 139.5, 135.5, 129.3, 127.9, 122.2, 112.1, 32.1, 26.2, 18.7, −3.9; positive ESIMS m/z (rel intensity) 521 (MNa^+, 100), 499 (MH^+, 82).

(*E*)-4-[3,5-Bis(*tert*-butyldimethylsilyloxy)styryl]phenol (13).[43] NaOMe (0.002 g, 0.038 mmol) was added to a well-stirred mixture of **12** (0.760 g, 1.52 mmol) in dry MeOH (2 mL) at room temperature. The resulting reaction mixture was stirred at room temperature for 2 h and concentrated under reduced pressure. The crude product was purified by column chromatography (eluent ether−hexanes 2:1, silica gel) to afford the product **13** as a clear oil (0.629 g, 92%). ^{1}H NMR (300 MHz, $CDCl_3$) δ 7.39 (d, J = 8.7 Hz, 2 H), 6.96 (d, J = 16.2 Hz, 1 H), 6.83 (d, J = 16.2 Hz, 1 H), 6.81 (d, J = 8.7 Hz, 2 H), 6.63 (d, J = 2.1 Hz, 2 H), 6.27 (t, J = 2.1 Hz, 1 H), 5.92 (s, 1 H), 1.00 (s, 18 H), 0.24 (s, 12 H); negative ESIMS m/z (rel intensity) 455 (100).

TBDMS-Protected Resveratrol Sodium 4′-Sulfate (14). $SO_3 \cdot$ pyridine (0.349 g, 2.189 mmol) was added to a well-stirred mixture of **13** (0.500 g, 1.095 mmol) in dry pyridine (2.0 mL) at room temperature under argon. The reaction mixture was heated to reflux under argon for 15 h. A solution of Na_2CO_3 (0.232 g, 2.189 mmol) in H_2O (2.0 mL) was added to the reaction mixture, which was stirred at 60 °C under argon for 1 h. The reaction mixture was cooled to room temperature and concentrated. The crude product was used directly for the next step, but the structure was confirmed by NMR. ^{1}H NMR (300 MHz, MeOH-d_4) δ 7.43 (d, J = 8.7 Hz, 2 H), 7.20 (d, J = 8.7 Hz, 1 H),

6.95 (d, J = 16.2 Hz, 1 H), 6.88 (d, J = 16.5 Hz, 1 H), 6.56 (d, J = 2.1 Hz, 2 H), 6.14 (t, J = 2.1 Hz, 1 H), 0.91 (s, 18 H), 0.13 (s, 12 H).

(*E*)-3-(*tert*-Butyldimethylsilyloxy)-5-[4-(*tert*-butyldimethylsilyloxy)styryl]phenol (15).[43] TBDMSCl (0.347 g, 2.300 mmol) was added to a well-stirred mixture of resveratrol (**1**, 0.500 g, 2.190 mmol) and imidazole (0.186 g, 2.738 mmol) in anhydrous DMF (2.0 mL) at −10 °C under argon. The reaction mixture was warmed to ambient temperature. After 12 h, additional imidazole (0.186 g, 2.738 mmol) and TBDMSCl (0.347 g, 2.300 mmol) were added to the reaction mixture and stirring was continued for 12 h. The resulting reaction mixture was diluted with EtOAc (80 mL) and washed with H_2O (3 × 30 mL). The combined organic layers were dried with sodium sulfate and concentrated. The resulting crude product was purified by flash column chromatography (eluent 10−25% hexanes−EtOAc, silica gel) to afford the product **15** as an orange oil (0.296 g, 33%). ^{1}H NMR (300 MHz, $CDCl_3$) δ 7.35 (d, J = 8.4 Hz, 2 H), 6.95 (d, J = 16.2 Hz, 1 H), 6.83−6.78 (m, 3 H), 6.57 (t, J = 1.5 Hz, 1 H), 6.53 (t, J = 1.8 Hz, 1 H), 6.24 (t, J = 2.1 Hz, 1 H), 5.24 (s, 1 H), 0.98 (s, 18 H), 0.20 (s, 12 H); negative ESIMS m/z (rel intensity) 455 (100).

(*E*)-3-(*tert*-Butyldimethylsilyloxy)-5-(4-hydroxystyryl)phenol (16).[43] Continuation of the column chromatography of **15** afforded **16** as an orange oil (0.113 g, 15%). ^{1}H NMR (300 MHz, $CDCl_3$) δ 7.37 (d, J = 8.4 Hz, 2 H), 6.95 (d, J = 16.2 Hz, 1 H), 6.83−6.78 (m, 3 H), 6.56 (t, J = 1.5 Hz, 1 H), 6.53 (t, J = 1.8 Hz, 1 H), 6.23 (t, J = 2.1 Hz, 1 H), 4.83 (s, 1 H), 4.71 (s, 1 H), 0.98 (s, 9 H), 0.20 (s, 6 H).

(*E*)-5-[4-(*tert*-Butyldimethylsilyloxy)styryl]benzene-1,3-diol (17).[43] Continuation of the column chromatography of **16** afforded **17** as a clear oil (0.090 g, 12%). ^{1}H NMR (300 MHz, $CDCl_3$) δ 7.32 (d, J = 8.7 Hz, 2 H), 6.94 (d, J = 16.2 Hz, 1 H), 6.81−6.76 (m, 3 H), 6.52 (d, J = 2.1 Hz, 2 H), 6.26 (t, J = 2.1 Hz, 1 H), 6.02 (s, 2 H), 0.98 (s, 9 H), 0.20 (s, 6 H); negative ESIMS m/z (rel intensity) 341 (100).

NFκB Luciferase Assay. Human embryonic kidney cells 293 were used to monitor any changes occurring along the NFκB pathway. This cell line contains chromosomal integration of a luciferase reporter construct regulated by the NFκB response element. Transcription factors can bind to the response element when stimulated by certain agents, allowing transcription of the luciferase gene. Following an incubation period of 48 h with TNFα and test compounds, cells were analyzed for luciferase activity using the Luc assay system from Promega.[49] Results were expressed as a percentage, relative to control (TNFα-treated) samples, and dose−response curves were constructed for the determination of IC_{50} values, which were generated from the results of five serial dilutions of test compounds and were the mean of two different experiments.

COX-1 and -2 Assays. COX-1 from sheep seminal vesicles and recombinant human COX-2 were purchased from Cayman Chemical, Ann Arbor, MI. The effect of test compounds on COX-1 and COX-2 was determined by measuring PGE_2 production produced in the COX reaction via an enzyme immunoassay. The reaction was initiated by adding arachidonic acid (AA). The mixture was incubated for 10 min at room temperature and terminated with 27.8 μM indomethecin. PGE_2 was quantitated by an ELISA method. Diluted samples of the reaction mixture were transferred to a 96-well plate (Nunc-Immuno Plate Maxisorp, Fisher Scientific, Pittsburgh, PA) coated with goat anti-mouse IgG (Jackson Immuno Research Laboratories, West Grove, PA). The tracer (PGE_2-acetylcholinesterase, Cayman Chemical, Ann Arbor, MI) and primary antibody (mouse anti-PGE_2, Monsanto, St. Louis, MO) were added. PGE_2 was determined by the spectrophotometric method at 412 nm using Elman's reagent. A standard curve with PGE_2 (Cayman Chemical, Ann Arbor, MI) was generated on the same plate, which was used to quantify the PGE_2 levels produced in the sample-treated wells. Results were expressed as a percentage, relative to control (solvent-treated) samples, and dose−response curves were generated for the determination of IC_{50} values.[87]

Measurement of Nitric Oxide (NO) Production in LPS-Stimulated Macrophages. This assay was performed as previously described.[88] Briefly, RAW 264.7 cells (1×10^5 cells/well) were incubated in 96-well culture plates for 24 h. The cells were treated with serially diluted compounds dissolved in phenol red-free DMEM for 30 min, followed by treatment with or without LPS (1 μg/mL) for an additional 20 h. NO is an unstable molecule and subsequently oxidized to a stable end product nitrite; therefore, the amount of NO was estimated by the measurement of nitrite. After 20 h, nitrite released in the media was reacted with Griess reagent, and absorbance was measured at 540 nm. A standard curve was created by using known concentrations of sodium nitrite.

NO-Scavenging Activity. Compounds were diluted 10 times with PBS, and 20 μL of the diluted solution of each compound was incubated with 100 μL of 6 mM SNP in PBS for 3 h at room temperature. The final concentration of compounds and SNP were 60 μM and 5 mM, respectively. The Griess reaction was performed to estimate the amount of nitrite. Briefly, 180 μL of Griess reagent was added in each well and the absorbance was measured at 540 nm.[89] The results are expressed as average of % inhibition of triplicate determinations ± standard deviation.

Western Blot Analysis. RAW 264.7 cells were pretreated with samples for 15 min before 1 μg/mL LPS for 18 h to examine the expression of iNOS protein. Cells were lysed with lysis buffer. Total protein (30 μg) in each cell lysate was resolved using 8% SDS−PAGE and electrotransferred to PVDF membranes. The membranes were incubated with 5% skimmed milk in 0.1% Tween-20 containing TBS (TBST) for 1 h at room temperature. Then membranes were incubated with corresponding primary antibodies in 3% skimmed milk in TBS for 1 h at 37 °C. After being washed with TBST for 5 min, three times, membranes were incubated with horse radish peroxidase (HRP) conjugated secondary antibodies for 1 h at 37 °C. Chemiluminescence (ECL) detection kit from Amersham Bioscience (Piscataway, NJ) was employed for the visualization according to the manufacturer's instructions.

Cell Cycle Analysis. HL-60 cells (2×10^5 cells/well) were treated with samples for 24 h. The medium was discarded, and nuclear isolation medium 4′,6-diamidino-2-phenylindole (NIM-DAPI; Beckman Coulter) solution was added just before the measurement using a Cell Lab Quanta SC (Beckman Coulter) flow cytometer. NIM-DAPI-stained cells were analyzed after excitation with UV light source. The distribution of cells in each phase of cell cycle was exhibited in a DNA histogram, and the percentage in sub-G_1 was analyzed.

Cytotoxicity with Cultured Cells. The effect of compounds on cancer cell proliferation was evaluated using the sulforhodamine B (SRB) method.[90] Briefly, KB or MCF7 cells were plated in 96-well plates containing samples and incubated at 37 °C in a humidified atmosphere with 5% CO_2. After 72 h of incubation, cells were fixed with 10% trichloroacetic acid solution for 1 h and stained with 0.4% SRB in 1% acetic acid solution. Stained cells were suspended in 10 mM Tris buffer. The effect of compounds on cell viability was quantified by measuring absorbance at 515 nm.

Tandem Mass Spectrometry of Resveratrol 4′-Sulfate. Negative ion electrospray mass spectrometry was used for the analysis of resveratrol 4′-sulfate (**7**) using a high resolution Waters Synapt QqTOF mass spectrometer. The deprotonated molecules of resveratrol and resveratrol 4′-sulfate (**7**) were abundant at m/z 227 and m/z 307, respectively, and were used as precursor ions for product ion tandem mass spectrometry. Resveratrol 4′-sulfate anion eliminated SO_3 to form a base peak of m/z 227 corresponding to resveratrol anion. Other abundant ions in the tandem mass spectra of resveratrol 4′-sulfate (**7**) and resveratrol were observed at m/z 185 and m/z 143. The transition of m/z 307 to m/z 227 was used during LC−MS−MS (using a Thermo Finnigan Quantum triple quadrupole mass spectrometer) with selected reaction monitoring (SRM) for the quantitative analysis

of resveratrol 4′-sulfate (**7**). The quantitative analysis of resveratrol in these studies was carried using SRM of the transition m/z 227 to m/z 185 as described previously.[31] Naringenin was used as an internal standard and measured by monitoring the SRM transition m/z 271 to m/z 151.

Stabilities of Resveratrol and Resveratrol 4′-Sulfate. The stabilities of resveratrol and resveratrol 4′-sulfate (**7**) were investigated for 24 h at 37 °C in RPMI 1640 (Invitrogen, Carlsbad, CA) cell culture medium which was used for the MCF-7 cellular uptake studies. These experiments were carried out three times. Resveratrol 4′-sulfate (**7**) was stable for 24 h (0 h, 100 ± 2.2%; 12 h, 95.1 ± 3.0%; 24 h, 98.8 ± 3.1%). However, resveratrol degraded ∼50% during 24 h under these conditions (0 h, 100 ± 0.3%; 12 h, 71.4 ± 7.2%; 24 h, 46.8 ± 8.7%).

Cellular Uptake Studies of Resveratrol and Resveratrol 4′-Sulfate. MCF7 human breast cancer cells (4.5×10^5 cells/well in a 96-well plate) were incubated with 50 μM resveratrol 4′-sulfate (**7**) at 37 °C for 24 h. The RPMI 1640 cell culture medium was removed, and the cells were rinsed three times with equal volumes of PBS. The cells in each well were harvested, treated with 120 μL of lysis buffer for 30 s with mixing, and then sonicated for 5 s. Acetonitrile (370 μL) and 10 μL of naringenin (internal standard, 20 μM) were added, and the cell lysate was vortex-mixed for 30 s. After centrifugation at 10000*g* at 4 °C for 15 min, the supernatant from each sample was removed, evaporated to dryness under a stream of nitrogen, and reconstituted in 100 μL of methanol/water (1:4) for analysis using LC−MS−MS. MCF-7 cells treated with resveratrol 4′-sulfate contained no resveratrol 4′-sulfate, resveratrol 3,5-disulfate, or resveratrol after 24 h. A negative control experiment in which the cells were treated with only buffer also showed no resveratrol or resveratrol sulfates in the cells. MCF-7 cells treated with resveratrol (positive control) were found to contain resveratrol (54.7 ± 19.0 pmol/million cells) and resveratrol 3,5-disulfate (1028.0 ± 166.6 pmol/million cells) but no resveratrol 4′-sulfate.

Inhibition of Aromatase. A high-throughput enzyme assay was used to screen samples for aromatase inhibition.[91] This assay employs dibenzylfuorescein as a substrate, and the level of fluorescence due to the resultant fluorescein indicates the level of enzyme activity.

Determination of QR Activity in Cell Culture. Quinone reductase was assessed using Hepa 1c1c7 murine hepatoma cells as previously reported.[81] Quinone reductase activity was measured as a function of the NADPH-dependent menadiol-mediated reduction of 3-(4,5-dimetylthiazo-2-yl)-2,5-diphenyltetrazolium bromide (MTT) to a blue formazan. Protein content was determined via crystal violet staining of identical plates. Specific activity is defined as nanomole of formazan formed per milligram of protein per minute. The induction ratio (IR) of QR activity represents the specific enzyme activity of agent-treated cells compared with a DMSO-treated control. The concentration to double activity (CD) was determined through a dose−response assay for active substances (IR > 2).

Evaluation of Antioxidant Capacity. To evaluate antioxidant capacity, 1,1-diphenyl-2-picrylhydrazyl (DPPH) free-radical scavenging was performed according to the method of Lee et al.[92] Briefly, 95 μL of DPPH radical solution (316 μM) was added in a 96-well plate containing 5 μL of each compound dissolved in 100% DMSO, and incubated for 30 min at 37 °C. The absorbance of each well was measured at 515 nm using a microplate reader. The DPPH radical scavenging activity of each sample was evaluated by calculating the percent of inhibition as follows: % inhibition = $(1 - A_{\text{sample}}/A_{\text{control}}) \times 100$.

Acknowledgment. This work was supported by Program Project Grant P01 CA48112 awarded by the National Cancer Institute.

References

(1) Jang, M.; Cai, L.; Udeani, G. O.; Slowing, K. V.; Thomas, C. F.; Beecher, C. W. W.; Fong, H. H. S.; Farnsworth, N. R.; Kinghorn, A. D.; Mehta, R. G.; Moon, R. C.; Mezzuto, J. M. Cancer Chemopreventive Activity of Resveratrol, a Natural Product Derived from Grapes. *Science* **1997**, *275*, 218–220.
(2) Bhat, K. P. L.; Pezzuto, J. M. Cancer Chemopreventive Activity of Resveratrol. *Ann. N.Y. Acad. Sci.* **2002**, *957*, 210–229.
(3) Pervaiz, S. Resveratrol: From Grapevines to Mammalian Biology. *FASEB J.* **2003**, *17*, 1975–1985.
(4) Kensler, T.; Guyton, K.; Egner, P.; McCarthy, T.; Lesko, S.; Akman, S. Role of Reactive Intermediates in Tumor Promotion and Progression. *Prog. Clin. Biol. Res.* **1995**, *391*, 103–116.
(5) Khanduja, K. L.; Bhardwaj, A.; Kaushik, G. Resveratrol Inhibits *N*-Nitrosodiethylamine-Induced Ornithine Decarboxylase and Cyclooxygenase in Mice. *J. Nutr. Sci. Vitaminol.* **2004**, *50*, 61–65.
(6) Kang, S. S.; Cuendet, M.; Endringer, D. C.; Croy, V. L.; Pezzuto, J. M.; Lipton, M. A. Synthesis and Biological Evaluation of a Library of Resveratrol Analogues as Inhibitors of COX-1, COX-2 and NF-κB. *Bioorg. Med. Chem.* **2009**, *17*, 1044–1054.
(7) Murias, M.; Handler, N.; Erker, T.; Pleban, K.; Ecker, G.; Saiko, P.; Szekeres, T.; Jager, W. Resveratrol Analogues as Selective Cyclooxygenase-2 Inhibitors: Synthesis and Structure−Activity Relationship. *Bioorg. Med. Chem.* **2004**, *12*, 5571–5578.
(8) Shigematsu, S.; Ishida, S.; Hara, M.; Takahashi, N.; Yoshimatsu, H.; Sakata, T.; Korthuis, R. J. Resveratrol, a Red Wine Constituent Polyphenol, Prevents Superoxide-Dependent Inflammatory Responses Induced by Ischemia/Reperfusion, Platelet-Activating Factor, or Oxidants. *Free Radical Biol. Med.* **2003**, *34*, 810–817.
(9) Ray, P. S.; Maulik, G.; Cordis, G. A.; Bertelli, A. A. E.; Bertelli, A.; Das, D. K. The Red Wine Antioxidant Resveratrol Protects Isolated Rat Hearts from Ischemia Reperfusion Injury. *Free Radical Biol. Med.* **1999**, *27*, 160–169.
(10) Wang, Y. J.; He, F.; Li, X. L. The Neuroprotection of Resveratrol in the Experimental Cerebral Ischemia. *Zhonghua Yixue Zazhi* **2003**, *83*, 534–536.
(11) Lu, K.-T.; Ko, M.-C.; Chen, B.-Y.; Huang, J.-C.; Hsieh, C.-W.; Lee, M.-C.; Chiou, R. Y. Y.; Wung, B.-S.; Peng, C.-Y.; Yang, Y.-L. Neuroprotective Effects of Resveratrol on MPTP-Induced Neuron Loss Mediated by Free Radical Scaenging. *J. Agric. Food Chem.* **2008**, *56*, 6910–6913.
(12) Bureau, G.; Longpre, F.; Martinoli, M. G. Resveratrol and Quercetin, Two Natural Polyphenols, Reduce Apoptotic Neuronal Cell Death Induced by Neuroinflammation. *J. Neurosci. Res.* **2008**, *86*, 403–410.
(13) Milne, J. C.; Lambert, P. D.; Schenk, S.; Carney, D. P.; Smith, J. J.; Gagne, D. J.; Jin, L.; Boss, O.; Perni, R. B.; Vu, C. B.; Bemis, J. E.; Xie, R.; Disch, J. S.; Ng, P. Y.; Nunes, J. J.; Lynch, A. V.; Yang, H. Y.; Galonek, H.; Israelian, K.; Choy, W.; Iffland, A.; Lavu, S.; Medvedik, O.; Sinclair, D. A.; Olefsky, J. M.; Jirousek, M. R.; Elliott, P. J.; Westphal, C. H. Small Molecule Activators of SIRT1 as Therapeutics for the Treatment of Type 2 Diabetes. *Nature* **2007**, *450*, 712–716.
(14) Howitz, K. T.; Bitterman, K. J.; Cohen, H. Y.; Lamming, D. W.; Lavu, S.; Wood, J. G.; Zipkin, R. E.; Chung, P.; Kisielewski, A.; Zhang, L. L.; Scherer, B.; Sinclair, D. A. Small Molecule Sctivators of Sirtuins Extend *Saccharomyces cerevisiae* Lifespan. *Nature* **2003**, *425*, 191–196.
(15) Valenzano, D. R.; Terzibasi, E.; Genade, T.; Cattaneo, A.; Domenici, L.; Cellerino, A. Resveratrol Prolongs Lifespan and Retards the Onset of Age-Related Markers in a Short-Lived Vertebrate. *Curr. Biol.* **2006**, *16*, 296–300.
(16) Rayalam, S.; Yang, J.-Y.; Ambati, S.; Della-Fera, M. A.; Baile, C. A. Resverarol Induces Apoptosis and Inhibits Adipogenesis in 3T3-L1 Adipocytes. *Phytother. Res.* **2008**, *22*, 1367–1371.
(17) Kapadia, G. J.; Azuine, M. A.; Tokuda, H.; Takasaki, M.; Mukainaka, T.; Konoshima, T.; Nishino, H. Chemopreventive Effect of Resveratrol, Sesamol, Sesame Oil and Sunflower Oil in the Epstein−Barr Virus Early Antigen Activation Assay and the Mouse Skin Two-Stage Carcinogenesis. *Pharmacol. Res.* **2002**, *45*, 499–505.
(18) Seya, K.; Kanemaru, K.; Sugimoto, C.; Suzuki, M.; Takeo, T.; Motomura, S.; Kitahara, H.; Niwa, M.; Oshima, Y.; Furukawa, K. I. Opposite Effects of Two Resveratrol (*trans*-3,5,4 Trihydroxystilbene) Tetramers, Vitisin A and Hopeaphenol, on Apoptosis of Myocytes Isolated from Adult Rat Heart. *J. Pharmacol Exp. Ther.* **2009**, *328*, 90–98.
(19) Dudley, J. I.; Lekli, I.; Mukherjee, S.; Das, M.; Bertelli, A. A. A.; Das, D. K. Does White Wine Qualify for French Paradox? Comparison of the Cardioprotective Effects of Red and White Wines and Their Constituents: Resveratrol, Tyrosol, and Hydroxytyrosol. *J. Agric. Food Chem.* **2008**, *56*, 9362–9373.

(20) Fremont, L. Minireview—Biological Effects of Resveratrol. *Life Sci*. **2000**, *66*, 663–673.
(21) Carbó, N.; Costelli, P.; Baccino, F. M.; López-Soriano, F. J.; Argilés, J. M. Resveratrol, a Natural Product Present in Wine, Decreases Tumour Growth in a Rat Tumour Model. *Biochem. Biophys. Res. Commun*. **1999**, *254*, 739–743.
(22) Roy, P.; Kalra, N.; Prasad, S.; George, J.; Shukla, Y. Chemopreventive Potential of Resveratrol in Mouse Skin Tumors through Regulation of Mitochondrial and PI3K/AKT Signaling Pathways. *Pharm. Res*. **2009**, *26*, 211–217.
(23) Aziz, M. H.; Kumar, R.; Ahmad, N. Cancer Chemoprevention by Resveratrol: In Vitro and in Vivo Studies and the Underlying Mechanisms (Review). *Int. J. Oncol*. **2003**, *23*, 17–28.
(24) Chen, Y.; Tseng, S. H.; Lai, H. S.; Chen, W. J. Resveratrol-Induced Cellular Apoptosis and Cell Cycle Arrest in Neuroblastoma Cells and Antitumor Effects on Neuroblastoma in Mice. *Surgery* **2004**, *136*, 57–66.
(25) Wenzel, E.; Soldo, T.; Erbersdobler, H.; Somoza, V. Bioactivity and Metabolism of *trans*-Resveratrol Orally Administered to Wistar Rats. *Mol. Nutr. Food Res*. **2005**, *49*, 482–494.
(26) De Santi, C.; Pietrabissa, A.; Spisni, R.; Mosca, F.; Pacifici, G. M. Sulphation of Resveratrol, a Natural Product Present in Grapes and Wine, in the Human Liver. *Xenobiotica* **2000**, *30*, 609–617.
(27) De Santi, C.; Pietrabissa, A.; Spisni, R.; Mosca, F.; Pacifici, G. M. Sulfation of Resveratrol, a Natural Compound Present in Wine, and Its Inhibition by Natural Flavonoids. *Xenobiotica* **2000**, *30*, 857–866.
(28) De Santi, C.; Pietrabissa, A.; Mosca, F.; Pacifici, G. M. Glucuronidation of Resveratrol, a Natural Product Present in Grape and Wine, in the Human Liver. *Xenobiotica* **2000**, *30*, 1047–1054.
(29) Kuhnle, G.; Spencer, J. P. E.;; Chowrimootoo, G.; Schroeter, H.; Debnam, E. S.; Srai, S. K. S.; Rice-Evans, C.; Hahn, U. Resveratrol Is Absorbed in the Small Intestine as Resveratrol Glucuronide. *Biochem. Biophys. Res. Commun*. **2000**, *272*, 212–217.
(30) Dyke, S. F.; Sainsbury, M.; Brown, D. W.; Palfreyman, M. N.; Wiggins, D. W. 1,2-Dihydroisoquinolines-XVI Indeno[1,2-*c*]isoquinoline Derivatives. *Tetrahedron* **1971**, *27*, 281–289.
(31) Yu, C. W.; Shin, Y. G.; Chow, A.; Li, Y. M.; Kosmeder, J. W.; Lee, Y. S.; Hirschelman, W. H.; Pezzuto, J. M.; Mehta, R. G.; van Breemen, R. B. Human, Rat, and Mouse Metabolism of Resveratrol. *Pharm. Res*. **2002**, *19*, 1907–1914.
(32) Vitrac, X.; Desmouliere, A.; Brouillaud, B.; Krisa, S.; Deffieux, G.; Barthe, N.; Rosenbaum, J.; Merillon, J. M. Distribution of [C-14]-*trans*-Resveratrol, a Cancer Chemopreventive Polyphenol, in Mouse Tissues After Oral Administration. *Life Sci*. **2003**, *72*, 2219–2233.
(33) Meng, X. F.; Maliakal, P.; Lu, H.; Lee, M. J.; Yang, C. S. Urinary and Plasma Levels of Resveratrol and Quercetin in Humans, Mice, and Rats After Ingestion of Pure Compounds and Grape Juice. *J. Agric. Food Chem*. **2004**, *52*, 935–942.
(34) Walle, T.; Hsieh, F.; DeLegge, M. H.; Oatis, J. E.; Walle, U. K. High Absorption but Very Low Bioavailability of Oral Resveratrol in Humans. *Drug Metab. Dispos*. **2004**, *32*, 1377–1382.
(35) Goldberg, D. A.; Yan, J.; Soleas, G. J. Absorption of Three Wine-Related Polyphenols in Three Different Matrices by Healthy Subjects. *Clin. Biochem*. **2003**, *36*, 79–87.
(36) Marier, J.-F.; Vachon, P.; Gritsas, A.; Zhang, J.; Moreau, J. P.; Ducharme, M. P. Metabolism and Disposition of Resveratrol in Rats: Extent of Absorption, Glucuronidation, and Enterohepatic Recirculation Evidenced by a Linked-Rat Model. *J. Pharmacol. Exp. Ther*. **2002**, *302*, 369–373.
(37) Li, Z. G.; Hong, T.; Shimada, Y.; Komoto, I.; Kawabe, A.; Ding, Y.; Kaganoi, J.; Hashimoto, Y.; Imamura, M. Suppression of *N*-Nitrosomethylbenzylamine (NMBA)-Induced Esophageal Tumorigenesis in F344 Rats by Resveratrol. *Carcinogenesis* **2002**, *23*, 1531–1536.
(38) Banerjee, S.; Bueso-Ramos, C.; Aggarwal, B. B. Suppression of 7,12-Dimethylbenz(*a*)anthracene-induced Mammary Carcinogenesis in Rats by Resveratrol: Role of Nuclear Factor-KappaB, Cyclooxygenase 2, and Matrix Metalloprotease 9. *Cancer Res*. **2002**, *62*, 4945–4954.
(39) Tessitore, L.; Davit, A.; Sarotto, I.; Caderni, G. Resveratrol Depresses the Growth of Colorectal Aberrant Crypt Foci by Affecting bax and p21(CIP) Expression. *Carcinogenesis* **2000**, *21*, 1619–1622.
(40) Terao, J. Dietary Flavonoids as Antioxidants in Vivo: Conjugated Metabolites of (−)-Epicatechin, and Quercetin Participate in Antioxidative Defense on Blood Plasma. *J. Med. Invest*. **1999**, *46*, 159–168.
(41) Moon, J.; Tsushida, T.; Nakahara, K.; Terao, J. Identification of Quercetin 3-*O*-beta-D-Glucoronide as an Antioxidative Metabolite in Rat Plasma after Oral Administration of Quercetin. *Free Radical Biol. Med*. **2001**, *30*, 1274–1285.
(42) Koga, T.; Meydani, M. Effect of Plasma Metabolites of (+)-Catechin and Quercetin on Monocyte Adhesion to Human Aortic Endothelial Cells. *Am. J. Clin. Nutr*. **2001**, *73*, 941–948.
(43) Zhang, Z.; Yu, B.; Schmidt, R. R. Synthesis of Mono- and Di-*O*-*β*-D-glucopyranoside Conjugaes of (*E*)-Resveratrol. *Synthesis* **2006**, 1301–1306.
(44) Orsini, F.; Pelizzoni, F.; Verotta, L.; Aburjai, T.; Rogers, C. B. Isolation, Synthesis, and Antiplatelet Aggregation Activity of Resveratrol 3-*O*-*β*-D-Glucopyranoside and Related Compounds. *J. Nat. Prod*. **1997**, *60*, 1082–1087.
(45) Yu, C.; Shin, Y. G.; Kosmeder, J. W.; Pezzuto, J. M.; van Breemen, R. B. Liquid Chromatography/Tandem Mass Spectrometric Determination of Inhibition of Human Cytochrome P450 Isozymes by Resveratrol and Resveratrol-3-sulfate. *Rapid Commun. Mass. Spectrom*. **2003**, *17*, 307–313.
(46) Farina, A.; Ferranti, C.; Marra, C. An Improved Synthesis of Resveratrol. *Nat. Prod. Res*. **2006**, *20*, 247–252.
(47) Raghuraman, A.; Riaz, M.; Hindle, M.; Desai, U. R. Rapid and Efficient Microwave-Assisted Synthesis of Highly Sulfated Organic Scaffolds. *Tetrahedron Lett*. **2007**, *48*, 6754–6758.
(48) Pezzuto, J. M. Resveratrol as an Inhibitor of Carcinogenesis. *Pharm. Biol*. **2008**, *46*, 443–573.
(49) Homhual, S.; Bunyapraphatsara, N.; Kondratyuk, T.; Herunsalee, A.; Chaukul, W.; Pezzuto, J. M.; Fong, H. H. S.; Zhang, H. J. Bioactive Dammarane Triterpenes from the Mangrove Plant *Bruguiera gymnorrhiza*. *J. Nat. Prod*. **2006**, *69*, 421–424.
(50) Kauffman, F. C.; Whittaker, M.; Anundi, I.; Thurman, R. G. Futile Cycling of a Sulfate Conjugate by Isolated Hepatocytes. *Mol. Pharmacol*. **1991**, *39*, 414–420.
(51) Nozawa, T.; Suzuki, M.; Yabuuchi, H.; Irokawa, M.; Tsuji, A.; Tamai, I. Suppression of Cell Proliferation by Inhibition of Estrone-3-sulfate Transporter in Estrogen-Dependent Breast Cancer Cells. *Pharm. Res*. **2005**, *22*, 1634–1641.
(52) Kwak, J. O.; Kim, H. W.; Oh, K. J.; Ko, C. B.; Park, H.; Cha, S. H. Characterization of Mouse Rrganic Anion Transporter 5 as a Renal Steroid Sulfate Transporter. *J. Steroid Biochem. Mol. Biol*. **2005**, *97*, 369–375.
(53) Mizuno, N.; Takahashi, T.; Iwase, Y.; Kusuhara, H.; Niwa, T.; Sugiyama, Y. Human Organic Anion Transporters 1 (hOAT1/SLC22A6) and 3 (hOAT3/SLC22A8) Transport Edaravone (MCI-186; 3-Methyl-1-phenyl-2-pyrazolin-5-one) and Its Sulfate Conjugate. *Drug Metab. Dispos*. **2007**, *35*, 1429–1434.
(54) Pezzuto, J. M.; Kosmeder, J.; Park, E. J.; Lee, S. K.; Cuendet, M.; Gills, J. J.; Bhat, K.; Grubjesic, S.; Park, H. S.; Mata-Greenwood, E.; Tan, Y.; Yu, R.; Lantvit, D. D.; Kinghorn, A. D. *Characterization of Natural Product Chemopreventive Agents*; Humana Press, Inc.: Totowa, NJ, 2005; Vol. 2, pp 3−37.
(55) Waffo-Teguo, P.; Hawthorne, M. E.; Cuendet, M.; Merillon, J.-M.; Kinghorn, A. D.; Pezzuto, J. M.; Mehta, R. G. Potential Cancer-Chemopreventive Activities of Wine Stilbenoids and Flavans Extracted from Grape (*Vitis vinifera*) Cell Cultures. *Nutr. Cancer* **2001**, *40*, 173–179.
(56) Watanabe, K.; Kawamori, T.; Nakatsugi, S.; Wakabayashi, K. COX-2 and iNOS, Good Targets for Chemoprevention of Colon Cancer. *BioFactors* **2000**, *12*, 129–133.
(57) Subbaramaiah, K.; Zakim, D.; Weksler, B. B.; Dannenberg, A. J. Inhibition of Cyclooxygenase: A Novel Approach to Cancer Prevention. *Proc. Soc. Exp. Biol. Med*. **1997**, *216*, 201–210.
(58) Kubatka, P.; Ahlers, I.; Ahlersova, E.; Adamekova, E.; Luk, P.; Bojkova, B.; Markova, M. Chemoprevention of Mammary Carcinogenesis in Female Rats by Rofecoxib. *Cancer Lett*. **2003**, *202*, 131–136.
(59) Nelson, J. E.; Harris, R. E. Inverse Association of Prostate Cancer and Non-Steroidal Anti-Inflammatory Dugs (NSAIDs): Results of a Case-Control Study. *Oncol. Rep*. **2000**, *7*, 169–170.
(60) Nakatsugi, S.; Ohta, T.; Kawamori, T.; Mutoh, M.; Tanigawa, T.; Watanabe, K.; Sugie, S.; Sugimura, T.; Wakabayashi, K. Chemoprevention by Nimesulide, a Selective Cyclooxygenase-2 Inhibitor, of 2-Amino-1-methyl-6-phenylimidazo[4,5-*b*]pyridine (PhIP)-Induced Mammary Gland Carcinogenesis in Rats. *Jpn. J. Cancer Res*. **2000**, *91*, 886–892.
(61) Kleinert, H.; Pautz, A.; Linker, K.; Schwarz, P. M. Regulation of the Expression of Inducible Nitric Oxide Synthase. *Eur. J. Pharmacol*. **2004**, *500*, 255–266.
(62) Jasnis, M. A.; Giri, J.; Davel, L. Nitric Oxide Is Involved in Stimulation of Tumor Growth. *Oncol. Rep*. **1997**, *4*, 1107–1111.
(63) Wadsworth, T. L.; Koop, D. R. Effects of the Wine Polyphenolics Quercetin and Resveratrol on Pro-Inflammatory Cytokine Expression in RAW 264.7 Macrophages. *Biochem. Pharmacol*. **1999**, *57*, 941–949.
(64) Tsai, S. H.; Lin-Shiau, S. Y.; Lin, J. K. Suppression of Nitric Oxide Synthase and the Down-Regulation of the Activation of NF

Kappa B in Macrophages by Resveratrol. *Br. J. Pharmacol.* **1999**, *126*, 673–680.
(65) Chan, M. M. Y.; Ho, C. T.; Huang, H. I. Effects of 3 Dietary Phytochemicals from Tea, Rosemary and Turmeric on Inflammation-Induced Nitrite Production. *Cancer Lett.* **1995**, *96*, 23–29.
(66) Kolodziej, H.; Radtke, O. A.; Kiderlen, A. F. Stimulus (Polyphenol, IFN-gamma, LPS)-Dependent Nitric Oxide Production and Antileishmanial Effects in RAW 264.7 Macrophages. *Phytochemistry* **2008**, *69*, 3103–3110.
(67) Aggarwal, B. B.; Shishodia, S. Molecular Targets of Dietary Agents for Prevention and Therapy of Cancer. *Biochem. Pharmacol.* **2006**, *71*, 1397–1421.
(68) Song, S. H.; Min, H. Y.; Han, A. R.; Nam, J. W.; Seo, E. K.; Park, S. W.; Lee, S. H.; Lee, S. K. Suppression of Inducible Nitric Oxide Synthase by (−)-Isoeleutherin from the Bulbs of *Eleutherine americana* through the Regulation of NF-Kappa B Activity. *Int. Immunopharmacol.* **2009**, *9*, 298–302.
(69) Djoko, B.; Chiou, R. Y. Y.; Shee, J. J.; Liu, Y. W. Characterization of Immunological Activities of Peanut Stilbenoids, Arachidin-1, Piceatannol, and Resveratrol on Lipopolysaccharide-Induced Inflammation of RAW 264.7 Macrophages. *J. Agric. Food Chem.* **2007**, *55*, 2376–2383.
(70) Whyte, L.; Huang, Y. Y.; Torres, K.; Mehta, R. G. Molecular Mechanisms of Resveratrol Action in Lung Cancer Cells Using Dual Protein and Microarray analyses. *Cancer Res.* **2007**, *67*, 12007–12017.
(71) Mahyar-Roemer, M.; Katsen, A.; Mestres, P.; Roemer, K. Resveratrol Induces Colon Tumor Cell Apoptosis Independently of p53 and Preceded by Epithelial Differentiation, Mitochondrial Proliferation and Membrane Potential Collapse. *Int. J. Cancer* **2001**, *94*, 615–622.
(72) Aziz, M. H.; Nihal, M.; Fu, V. X.; Jarrard, D. F.; Ahmad, N. Resveratrol-Caused Apoptosis of Human Prostate Carcinoma LNCaP Cells is Mediated via Modulation of Phosphatidylinositol 3′-Kinase/Akt Pathway and Bcl-2 Family Proteins. *Mol. Cancer Ther.* **2006**, *5*, 1335–1341.
(73) Scarlatti, F.; Sala, G.; Somenzi, G.; Signorelli, P.; Sacchi, N.; Ghidoni, R. Resveratrol Induces Growth Inhibition and Apoptosis in Metastatic Breast Cancer Cells via De Novo Ceramide Signaling. *FASEB J.* **2003**, *17*, 2339–2341.
(74) Puissant, A.; Grosso, S.; Jacquel, A.; Belhacene, N.; Colosetti, P.; Cassuto, J. P.; Auberger, P. Imatinib Mesylate-Resistant Human Chronic Myelogenous Leukemia Cell Lines Exhibit High Sensitivity to the Phytoalexin Resveratrol. *FASEB J.* **2008**, *22*, 1894–1904.
(75) Murray, R. Role of Anti-Aromatase Agents in Postmenopausal Advanced Breast Cancer. *Cancer Chemother. Pharmacol.* **2001**, *48*, 259–265.
(76) Ghosh, S.; Choudary, A.; Musi, N.; Hu, Y. F.; Li, R. IKK Beta Mediates Cell Shape-Induced Aromatase Expression and Estrogen Biosynthesis in Adipose Stromal Cells. *Mol. Endocrinol.* **2009**, *23*, 662–670.
(77) Tong, K. I.; Katoh, Y.; Kusunoki, H.; Itoh, K.; Tanaka, T.; Yamamoto, M. Keap1 Recruits Neh2 through Binding to ETGE and DLG Motifs: Characterization of the Two-Site Molecular Recognition Model. *Mol. Cell. Biol.* **2006**, *26*, 2887–2900.
(78) Talalay, P.; Fahey, J. W.; Holtzclaw, W. D.; Prestera, T.; Zhang, Y. S. Chemoprotection against Cancer by Phase 2 Enzyme Induction. *Toxicol. Lett.* **1995**, *82*−*3*, 173–179.
(79) Nho, C. W.; Jeffery, E. The Synergistic Upregulation of Phase II Detoxification Enzymes by Glucosinolate Breakdown Products in Cruciferous Vegetables. *Toxicol. Appl. Pharmacol.* **2001**, *174*, 146–152.
(80) Kennelly, E. J.; Gerhauser, C.; Song, L. L.; Graham, J. G.; Beecher, C. W. W.; Pezzuto, J. M.; Kinghorn, A. D. Induction of Quinone Reductase by Withanolides Isolated from *Physalis philadelphica* (tomatillos). *J. Agric. Food Chem.* **1997**, *45*, 3771–3777.
(81) Song, L. L.; Kosmeder, J. W., II; Lee, S. K.; Gerhäuser, C.; Lantvit, D.; Moon, R. C.; Moriarty, R. M.; Pezzuto, J. M. Cancer Chemopreventive Activity Mediated by 4′-Bromoflavone, a Potent Inducer of Phase II Detoxication Enzymes. *Cancer Res.* **1999**, *59*, 578–585.
(82) Prochaska, H. J.; Santamaria, A. B. Direct Measurement of Nad(P)H−Quinone Reductase from Cells Cultured in Microtiter Wells—A Screening Assay for Anticarcinogenic Enzyme Inducers. *Anal. Biochem.* **1988**, *169*, 328–336.
(83) Qian, Y. P.; Cai, Y. J.; Fan, G. J.; Wei, Q. Y.; Yang, J.; Zheng, L. F.; Li, X. Z.; Fang, J. G.; Zhou, B. Antioxidant-Based Lead Discovery for Cancer Chemoprevention: The Case of Resveratrol. *J. Med. Chem.* **2009**, *52*, 1963–1974.
(84) Saiko, P.; Szakmary, A.; Jaeger, W.; Szekeres, T. Resveratrol and Its Analogs: Defense against Cancer, Coronary Disease and Neurodegenerative Maladies or Just a Fad? *Mutat. Res.* **2008**, *658*, 68–94.
(85) de la Lastra, C. A.; Villegas, I. Resveratrol as Antioxidant and Pro-Oxidant Agent: Mechanism and Clinical Implications. *Biochem. Soc. Trans.* **2007**, *35*, 1156–1160.
(86) Kundu, J. K.; Surh, Y. J. Cancer Chemopreventive and Therapeutic Potential of Resveratrol: Mechanistic Perspectives. *Cancer Lett.* **2008**, *269*, 243–261.
(87) Cuendet, M.; Mesecar, A. D.; DeWitt, D. L.; Pezzuto, J. M. An ELISA Method To Measure Inhibition of the COX Enzymes. *Nat. Protocol.* **2006**, *1*, 1915–1921.
(88) Asolkar, R. N.; Freel, K. C.; Jensen, P. R.; Fenical, W.; Kondratyuk, T. P.; Park, E. J.; Pezzuto, J. M. Arenamides A−C, Cytotoxic NF Kappa B Inhibitors from the Marine Actinomycete *Salinispora arenicola*. *J. Nat. Prod.* **2009**, *72*, 396–402.
(89) Tsai, P. J.; Tsai, T. H.; Yu, C. H.; Ho, S. C. Comparison of NO-Scavenging and NO-Suppressing Activities of Different Herbal Teas with Those of Green Tea. *Food Chem.* **2007**, *103*, 181–187.
(90) Skehan, P.; Storeng, R.; Scudiero, D.; Monks, A.; McMahon, J.; Vistica, D.; Warren, J. T.; Bokesch, H.; Kenney, S.; Boyd, M. R. New Colorimetric Cytotoxicity Assay for Anticancer-Drug Screening. *J. Natl. Cancer Inst.* **1990**, *82*, 1107–1112.
(91) Lee, D.; Bhat, K. P. L.; Fong, H. H. S.; Farnsworth, N. R.; Pezzuto, J. M.; Kinghorn, A. D. Aromatase Inhibitors from *Broussonetia papyrifera*. *J. Nat. Prod.* **2001**, *64*, 1286–1293.
(92) Lee, S. K.; Mbwambo, Z. H.; Chung, H. S.; Luyengi, L.; Gamez, E. J. C.; Mehta, R. G.; Kinghorn, A. D.; Pezzuto, J. M. Evaluation of the Antioxidant Potential of Natural Products. *Comb. Chem. High Throughput Screening* **1998**, *1*, 35–46.